

First Announcement (updated) / Call for Papers

# **The 1<sup>st</sup> International Conference on Automobile Steel (ICAS2016)**

# **The 3<sup>rd</sup> International Conference on High Manganese Steels ( HMnS2016)**

**Chengdu, China**

**November 16-18, 2016**

[\*\*www.icas-2016.com\*\*](http://www.icas-2016.com)

[\*\*hmns2016.csm.org.cn\*\*](http://hmns2016.csm.org.cn)

**Organized by**

The Chinese Society for Metals

Central Iron and Steel Research Institute

# Effects of Strain Rate and Temperature on the Mechanical Properties of Medium Manganese Steels

RANA Radhakanta<sup>\*</sup>, MATLOCK David, SPEER John, DE MOOR Emmanuel

(Advanced Steel Processing and Products Research Center, Colorado School of Mines, Golden, Colorado 80401, USA;

<sup>\*</sup>Currently at Tata Steel R&D, 1970CA IJmuiden, The Netherlands)

**Abstract:** The effects of temperature (-60 to 100 °C) and strain rate (0.002 to 0.2 s<sup>-1</sup>) on the properties of Al-alloyed 7 and 10 wt-% Mn steels containing 34.8 and 57.3 vol-% austenite respectively were evaluated by tensile tests in isothermal liquid baths. The tensile strengths of both medium Mn steels increased with a decrease in temperature owing to the decreased austenite stability with a decrease in temperature. At lower temperatures the strength of the 10MnAl steel was highest, a consequence of the higher strain hardening rate caused by more austenite transformation to martensite with deformation. The resulting properties are assessed with a consideration of the effects of strain rate and deformation on adiabatic heating which was observed to be as high as 95 °C.

**Key words:** austenite stability, strain rate, temperature, mechanical properties

Medium Mn steels are a class of 3<sup>rd</sup> generation advanced high strength steels (3GAHSS) that contain Mn, usually in the range of 5-12 wt-%<sup>[1]</sup>. These steels exhibit very high tensile elongations (>30%) at high strengths (tensile strengths >800 MPa) which reflect strengthening and strain stabilization during deformation due to transformation of retained austenite (typically present with amounts >20 vol.%) to martensite, *i.e.* the transformation induced plasticity (TRIP) effect. Austenite stabilization is primarily a result of Mn partitioning into austenite during intercritical annealing or other processing histories and is anticipated to be highly temperature dependent, increasing with an increase in test temperature.

During forming of automotive steel sheets, the actual sheet temperature is typically greater than ambient due to the effects of friction and adiabatic heating which are enhanced at the typical high strain rates imposed during forming<sup>[2]</sup>. As shown in a recent study on a metastable austenitic stainless steel, the stability of austenite depends on strain rate and temperature<sup>[3]</sup>, implying that the mechanical properties of medium Mn steels with metastable austenite evolve during forming and the final properties reflect the combined effects of strain, strain rate, and temperature. Therefore, the current study was undertaken to assess the effects of strain

rate and temperature on the mechanical properties of medium Mn steels.

## 1 Experimental Method

Two medium Mn steels, 7MnAl (7.4Mn-1.55Al-0.14C-0.2Si, wt-%) and 10MnAl (10.1Mn-1.68Al-0.14C-0.2Si, wt-%), were thermomechanically processed to 1.5 mm, with a final cold rolling reduction of 62.4%<sup>[1]</sup>. To produce microstructures with significant amounts of retained austenite, the cold rolled steels were annealed at 640 °C for 16 h and then air-cooled to room temperature. ASTM E-8 sub-sized tensile specimens were machined from the annealed material and tested at -60, -20, 20, 60 and 100 °C with engineering strain rates of 0.002, 0.02 and 0.2 s<sup>-1</sup>. Tensile strains were measured with a special submersible extensometer which measured strains to failure in a 25.4 mm gage length. To minimize adiabatic heating, tensile specimens for tests at -60 to 20 °C were immersed in controlled-temperature ethanol baths and specimens tested at 60 and 100 °C were immersed in oil baths preheated to the required temperatures. In addition, tests at ambient temperature were conducted in air to contrast the effect of the liquid environment on the extent of adiabatic heating. For this purpose, K-type thermocouples were spot-welded to the specimens in the gage area to monitor temperature

changes during testing. Mechanical properties were obtained using tensile tests to failure; tensile tests interrupted at 20% engineering strain were used to determine austenite stability, *i.e.* the effects of test temperature and strain rate on austenite transformation to martensite. An engineering strain of 20% was selected as a characteristic strain value within the uniform strain range of all test specimens.

Austenite contents were measured by X-ray diffraction (XRD) using Cu-K $\alpha$  radiation. Samples for XRD were prepared by metallographic grinding followed by chemical dissolution for at least 300 s in a solution of H<sub>2</sub>O, H<sub>2</sub>O<sub>2</sub> and HF (10:10:1 by volume). The amount of austenite was determined following the SAE Intl. method<sup>[4]</sup>.

Microstructures of selected samples were observed in a field emission scanning electron microscope (FESEM) using secondary electron imaging mode with 5 kV accelerating voltage. Metallographic specimens for FESEM were etched with 2 vol-% nital solution. Deformed samples were from the uniform deformation area of the gage section after final fracture.

In this paper selected results from the experiments on the two steels are presented. A more complete discussion of the results is presented elsewhere<sup>[5]</sup>.

## 2 Typical Results and Discussion

### 2.1 Adiabatic heating

Figure 1a compares the maximum temperature increases as a function of strain rate in the 7MnAl steel tested in air and ethanol at 20 °C. The  $\Delta T_{\max}$  values increased with strain rate and the magnitudes were higher for samples tested in air. The highest value of  $\Delta T_{\max}$  was 95 °C for the strain rate of 0.2 s<sup>-1</sup> and near-isothermal conditions were only obtained for the sample tested in ethanol at a strain rate of 0.002 s<sup>-1</sup>. Figure 1b shows that the extent of the temperature rise with strain rate was essentially independent of test temperature for samples tested in isothermal baths over the temperature range of this study.

Adiabatic heating during deformation results from insufficient time for the thermal energy generated to dissipate, an effect which increased with strain rate. The substantial adiabatic heating in the medium Mn steels studied here also reflects their reduced thermal

conductivity due to the presence of large austenite fractions in the microstructures (as discussed below), and relatively high alloy contents<sup>[6]</sup>. Immersion of the samples in a liquid bath during deformation enhanced heat dissipation to the surroundings, resulting in a decrease in the extent of adiabatic heating.

### 2.2 Microstructure and austenite stability

Figure 2a shows a representative as-annealed microstructure for the 10MnAl steel and Figs. 2b and 2c respectively show the deformed and transformed microstructures after 20% engineering strain at -60 °C and 100 °C at a strain rate of 0.2 s<sup>-1</sup>. In the annealed condition (Fig. 2a) the ultrafine (1-2  $\mu$ m grain size) microstructure consists of ferrite (dark grey), austenite (lighter constituent with less surface relief) and martensite or martensite-austenite (M-A) constituents (evident by regions with higher surface relief). In the deformed samples, the martensite phase fraction appeared greater after deformation and to a greater extent in the sample tested at -60 °C than for the sample deformed at 100 °C, owing to the temperature sensitivity of the TRIP effect.

The austenite contents in the annealed samples were determined by XRD as 34.8 and 57.3 vol-% in the 7MnAl and 10MnAl steels respectively. To quantitatively compare austenite stability in the steels, a parameter, the “austenite transformation ratio,” was defined as the ratio of the amount of austenite transformed to the initial austenite amount and determined for each of the testing conditions. An austenite transformation ratio of 1 indicates that all initial austenite transformed at strains less than 20% engineering strain, and a ratio of 0 indicates no austenite transformation.

Figures 3a and 3b respectively show for both the 7MnAl and 10MnAl steels that the austenite transformation ratios decreased with an increase in test temperature and were essentially independent of strain rate over the range evaluated. Thus, the austenite stability for both steels increased with increasing test temperature (*i.e.* the austenite transformation ratio decreased from approximately 0.6-0.85 at -60 °C to as low as 0.2-0.45 at 100 °C). At low temperatures (-60 to 20 °C), the austenite stability was similar for both steels. At higher test temperatures (60 to 100 °C), the

increase in austenite stability was greater for the 10MnAl steel (Fig. 3b) than for the 7MnAl steel (Fig. 3a). The observed differences in austenite stability between the 7MnAl and 10MnAl steels suggest that in addition to initial austenite volume fraction Mn

partitioning and distribution in austenite also affects the observed temperature-dependent stability. Further work will be required to assess completely the effects of compositional differences and gradients on stability against deformation-induced transformation.

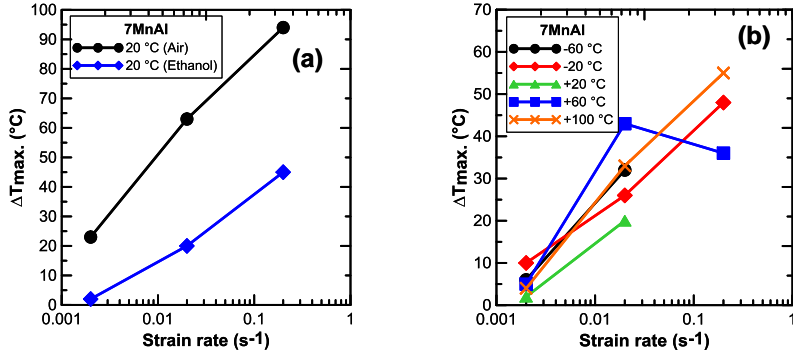


**Fig. 1 Maximum temperature rise of tensile specimens due to adiabatic heating ( $\Delta T_{\max}$ ) during testing of 7MnAl steel**

a—comparison of the  $\Delta T_{\max}$  for ambient temperature (20 °C) tensile tests with different strain rates in air and ethanol; b—the  $\Delta T_{\max}$  during tensile tests with various strain rates and test temperatures tested in isothermal baths

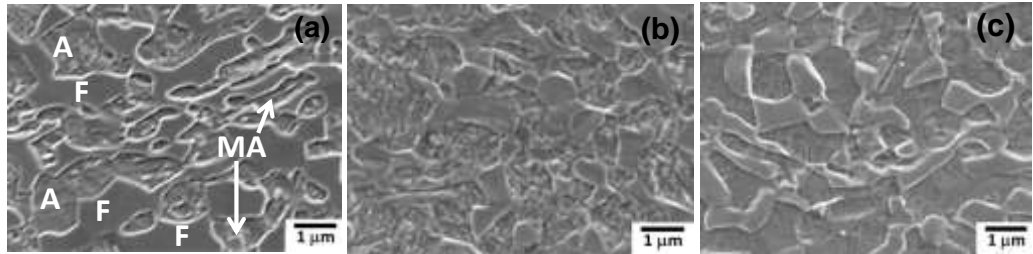


**Fig. 2 Representative 10MnAl steel microstructural (FESEM, thickness section) changes due to deformation in isothermal baths.**

a—as-annealed (undeformed); b—deformed to 20% strain at -60 °C with 0.2  $\text{s}^{-1}$  strain rate; c—deformed to 20% strain at 100 °C with 0.2  $\text{s}^{-1}$  strain rate

### 2.3 Mechanical properties

Figure 4a shows engineering stress-strain curves for the 10MnAl steel tested at different temperatures and at a constant strain rate. These curves are similar to the results obtained for both steels at all strain rates. The shapes of the tensile curves in Fig. 4a indicate that the strain hardening rate increased with a decrease in test temperature due to the decrease in austenite stability shown in Fig. 3b resulting in intensive strain-induced transformation to martensite at lower temperatures.

Figures 4b and 4c summarize the effects of test temperature and strain rate on the ultimate tensile strengths (UTS) for the 7MnAl and 10MnAl steels respectively. Both steels exhibit a significant decrease in UTS with an increase in temperature; the temperature-dependent behavior is essentially independent of strain rate over the strain rate range

considered here. The UTS values at all temperatures for the 7MnAl steel were lower than the corresponding values for the 10MnAl steel, a consequence of the higher strain hardening rate in the latter steel caused by a more pronounced TRIP effect owing to the presence of a higher initial austenite fraction and extensive transformation to martensite. For both steels the lower UTS values at the high temperatures reflected the increased austenite stability at higher temperatures. In general, a higher strain rate in both the steels resulted in decrease in UTS due to adiabatic heating during testing (Fig. 1). However, the effect of temperature on the strength appeared to be stronger than that of strain rate over the range of test temperatures and strain rates used in this study. Further, the temperature effect on UTS was more pronounced in the 10MnAl steel than the 7MnAl steel, interpreted to be due to the higher initial amount of austenite present in the 10MnAl steel.

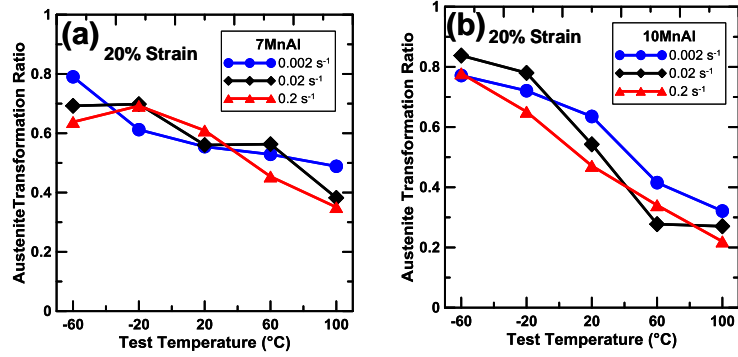


Fig. 3 Austenite transformation ratio at 20% engineering strain as function of test temperature (-60 to 100 °C) of the steels tested in isothermal baths in the strain rate range of 0.002-0.2 s<sup>-1</sup>

a—7MnAl; b—10MnAl

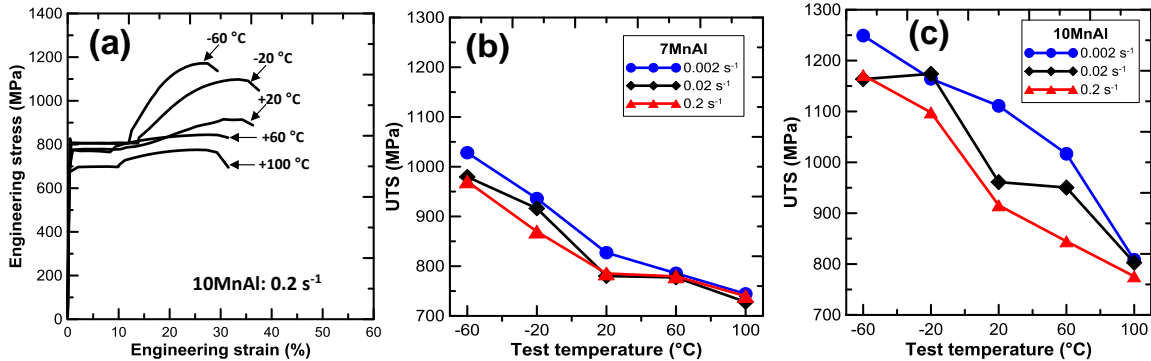


Fig. 4 Typical tensile behavior of the steels tested under conditions of varying strain rate and temperature

a—representative engineering stress-strain curves of 10MnAl steel tested with a strain rate of 0.2 s<sup>-1</sup>; b—variation of tensile strength of 7MnAl steel; c—variation of tensile strength of 10MnAl steel

### 3.0 Conclusions

(1) The temperature-dependent tensile properties of the medium Mn steels considered here are sensitive to the stability of austenite against transformation to martensite with strain.

(2) Austenite stability increases with temperature, applied or due to adiabatic heating, leading to significant decreases in strength with an increase in temperature.

(3) The extent of adiabatic heating increases with an increase in strain rate over the range of strain rates considered here.

(4) Tensile tests in isothermal baths minimize but do not eliminate the effects of adiabatic heating for the medium Mn steels.

### References:

- [1] Gibbs P J, *et al.* Austenite stability effects on tensile behavior of manganese enriched austenite transformation induced plasticity steel [J]. *Metall. Mater. Trans. A*, 2011, 42(12): 3691~3702.
- [2] Kapoor R, Nemat-Naser J C, Determination of temperature rise during high strain rate deformation [J]. *Mech. Mater.*, 1991, 27(1):1~12.
- [3] Tsuchida N, *et al.* Effects of temperature and strain rate on TRIP effect in SUS301L metastable austenitic stainless steel [J]. *ISIJ Inter.*, 2013, 53(10):1881~1887.
- [4] Jatczak C, Retained austenite and its measurement by X-ray diffraction [M]. *SAE Tech Paper 800426*, 1980.
- [5] R Rana *et al.* “Temperature and strain rate dependent properties of medium Mn steels,” Colorado School of Mines, 2016, in preparation for publication.
- [6] Peet M J, *et al.* Prediction of thermal conductivity of steel [J]. *Inter. J. Heat Mass Transf.*, 2011, 54(11-12):2602~2608.

*This material is based upon work supported by the Department of Energy National Energy Technology Laboratory under Award Number(s) DE-EE0005976.*

*This report was prepared as an account of work sponsored by an agency of the United States Government. Neither the United States Government nor any agency thereof, nor any of their employees, makes any warranty, express or implied, or assumes any legal liability or responsibility for the accuracy, completeness, or usefulness of any information, apparatus, product, or process disclosed, or represents that its use would not infringe privately owned rights. Reference herein to any specific commercial product, process, or service by trade name, trademark, manufacturer, or otherwise does not necessarily constitute or imply its endorsement, recommendation, or favoring by the United States Government or any agency thereof. The views and opinions of authors expressed herein do not necessarily state or reflect those of the United States Government or any agency thereof.*